CSIRO PUBLISHING www.publish.csiro.au/journals/eg Copublished paper, please cite all three:
Exploration Geophysics, 2011, **42**, 69–79; *Butsuri-Tansa*, 2011, **64**, 69–79; *Jigu-Mulli-wa-Mulli-Tamsa*, 2011, **14**, 69–79

Estimation of site amplification and S-wave velocity profiles in metropolitan Manila, the Philippines, from earthquake ground motion records

Hiroaki Yamanaka[1,3] Kaoru Ohtawara[1] Rhommel Grutas[1] Robert B. Tiglao[2]
Melchor Lasala[2] Ishmael C. Narag[2] Bartlome C. Bautista[2]

[1]The Interdisciplinary Graduate School of Science and Engineering, Tokyo Institute of Technology, 4259 Nagatsuta, Midori-ku, Yokohama, Japan.
[2]Philippine Institute of Volcanology and Seismology, CP Garcia Avenue, UP Campus, Diliman, Quezon City, the Philippines.
[3]Corresponding author. Email: yamanaka@depe.titech.ac.jp

Abstract. In this study, empirical site amplifications and S-wave velocity profiles for shallow and deep soils are estimated using earthquake ground motion records in metropolitan Manila, the Philippines. We first apply a spectral inversion technique to the earthquake records to estimate effects of source, path, and local site amplification. The earthquake data used were obtained during 36 moderate earthquakes at 10 strong-motion stations of an earthquake observation network in Manila. The estimated Q value of the propagation path is modelled as $54.6f^{1.1}$. Most of the source spectra can be approximated with the omega-square model. The site amplifications show characteristic features according to surface geological conditions. The amplifications at the sites in the coastal lowland and Marikina Valley shows predominant peaks at frequencies from 1 to 5 Hz, while those in the central plateau are characterised by no dominant peaks. These site amplifications are inverted to subsurface S-wave velocity. We, next, discuss the relationship between the amplifications and average S-wave velocity in the top 30 m of the S-wave velocity profiles. The amplifications at low frequencies are well correlated with the averaged S-wave velocity. However, high-frequency amplifications cannot be sufficiently explained by the averaged S-wave velocity in the top 30 m. They are correlated more with the average of S-wave velocity over depths less than 30 m.

Key words: earthquake observation, Manila, site amplification, S-wave velocity, Q-value, the Philippines.

Introduction

Metropolitan Manila, the Philippines, is one of the typical mega-cities in Asia, with a large population of more than 10 million people, and various kinds of buildings including many high-rise buildings. This city is located on Luzon Island, which is characterised by a special tectonic setting. It is sandwiched by the Philippine Sea Plate to the east, and the Eurasian Plate to the west. This tectonic setting makes the region one of the high seismicity areas in the world. Furthermore, an active fault system (Valley Fault) has been identified in the vicinity of metropolitan Manila (Daligdig et al., 1997). A paleoseismological investigation indicated that this fault generated 2–4 events in the past 2600 years (Nelson et al., 2000). They also suggested that the active fault might generate an earthquake with a magnitude of 6–7. Therefore, disaster mitigation is one of the important issues in metropolitan Manila due to this geological setting and social interest. Accordingly, several seismic zoning maps have been already proposed for metropolitan Manila (e.g. Daligdig and Besana, 1993; Philippine Institute of Volcanology and Seismoloy, 2004). In the zonation maps, high seismic intensity has been predicted in areas with soft soils, due to amplification effects. It is well known that the distribution of earthquake ground motion in a basin is significantly controlled by amplification effects due to local geological conditions. Therefore, such effects of geological conditions must be accurately included in a reliable estimation of strong ground motion during a future large event. Although many relationships between amplification factors and geological or geomorphological conditions are available for seismic zonation work, we must validate and localise such relations for use in a target area using actual observed ground motion data.

A strong motion observation network was deployed in metropolitan Manila in 1998 to accumulate fundamental data for assessing strong ground shaking including local geological effects in the area (Kurita et al., 2000), and has been operated by the Philippine Institute of Volcanology and Seismoloy (PHIVOLCS) in a cooperation with the earthquake engineering group at Tokyo Institute of Technology. This was the first systematic strong-motion observation network installed at locations with various geological conditions in the area. It has been shown from the observed data that the shallow soil layers (to 60 m) and deep Tertiary sedimentary layers (to 2 km) in the area affect strong ground motion in a wide frequency range (Yamanaka et al., 2002*a*).

In this study, we have estimated site amplifications by applying a spectral inversion technique to earthquake ground motion records from metropolitan Manila. Then, we have calculated S-wave velocity profiles from an inversion of the amplification factors. We have finally estimated relationships between the local site amplifications and the S-wave velocity structure of sedimentary layers in the area.

 10.1071/EG11003 0812-3985/11/010069

Geological conditions

The target area in this study, metropolitan Manila, is shown in the elevation map in Figure 1. Surface geological conditions in the area are roughly divided into four categories (e.g. Gervasio, 1968). The coastal area along Manila Bay in the west is covered with soft Quaternary layers with a maximum thickness of ~50 m (e.g. Daligdig and Besana, 1993). It is expected that the Quaternary layers will amplify high-frequency ground motion. The soft layers become thinner towards the central plateau, which is characterised by high elevations to the east of the coastal area. The surface geological formations in the central plateau consist of stiff soils including tuff layers near the surface. The tuff formation is regarded as engineering bedrock with low or no site amplification in the previous zoning map (Daligdig and Besana, 1993). The Marikina Valley to the east of the central plateau is a pull-apart basin caused by the western and eastern Valley Faults. The valley is also covered with soft soils of Quaternary age. In particular the soft soils increase in thickness to the south near the Laguna de Bay. The most eastern part of the target area is part of the Sierra Madre Mountains, and is classified as a rock area where the basement appears near the surface beneath weathered layers.

The shallow Quaternary layer features mentioned above have been well understood in metropolitan Manila (e.g. Gervasio, 1968). However, the structure of deep sedimentary layers over the basement, with an S-wave velocity of ~3 km/s, is not well known. Yamanaka et al. (2002*b*) conducted microtremor-array exploration to reveal the S-wave velocity profiles of the deep sedimentary layers over the basement. They found that the thickness of the Tertiary deep soils is 1 to 2 km in metropolitan Manila, except in the mountain area in the east.

Earthquake observation and ground motion records

Earthquake observation

Strong-motion earthquake observations in metropolitan Manila have been conducted since 1998 (Kurita et al., 2000). The 10 stations serve the four geological areas as shown in Figure 1. Four stations are located in the coastal lowland. PSY is close to the coast of Manila Bay, while UST is located near the boundary between the coastal area and the central plateau. Three sites are located in the central plateau, and MKT and ORT are stations located in business areas with many high-rise buildings. Two stations, MRK and PAT, were deployed in the Marikina Valley. SKB is located in the Sierrra Madre mountain area, and served as a reference site to estimate site amplification effects in this study. A strong-motion accerelograph was installed at each station.

Earthquake data

The earthquake data used were obtained during 36 moderate earthquakes observed at the 10 strong-motion stations network from 1995 to 2005. The epicentres of the events are shown in Figure 1. The magnitudes of the events are 2.5 to 6.8, and the focal depths are 1 to 153 km, determined by PHIVOLCS and tabulated in Table 1. Figure 2*a* shows the distributions of the hypocenters projected onto an east-to-west line. Shallow events occurred in the east and are related with the Philippine Fault, while the deep events occurred along the subducting plate. The hypocentral distances for all the sites are from 30 to 250 km as shown in Figure 2*b*. A total of 189 records were used in this study. The peak ground accelerations in the records are less than 100 cm/s^2, and corresponding ground velocities are less than 10 cm/s, as can be seen in Figure 3. Therefore, soils at all the sites would have behaved linearly during the earthquakes discussed in this study.

The procedure for calculating S-wave spectra is as follows. First, we estimated arrival times of S-wave onsets in the earthquake records, in order to choose segments with a duration of 10 s containing S-wave energy. Horizontal spectra were then calculated from each of the horizontal components of motion, using the Fast Fourier Transform on the tapered data from the selected windows. We next obtained a spectrum from the root-mean-square combination of the two horizontal spectra. Examples of the earthquake ground motion and the spectra are shown in Figures 4 and 5. The spectrum at PSY is the largest in magnitude, while that at SKB is small except for the peak at a frequency of ~10 Hz.

Spectral inversion for site effects

Constraint condition

We used the spectral inversion technique by Iwata and Irikura (1986) to separate the effects of source, propagation path, and site amplification from the S-wave spectra. The method requires a constraint to solve the governing equations. Iwata and Irikura (1986) used a constraint condition in which amplifications at all the sites were more than two, considering the surface effects. Kato et al. (1992) used a constraint condition that amplification factor is two at a rock site at each frequency. Takemura et al. (1991) and Yamanaka et al. (1998) applied constraint conditions calculated numerically, considering actual topographic features or 1D amplification for a soil model at a reference site.

In this study, a constraint condition similar to that of Yamanaka et al. (1998) was used by defining the theoretical 1D amplification of S-waves at the reference site of SKB. As explained above this site is in a rock area that is covered with near-surface weathered layers. These shallow soils can amplify ground

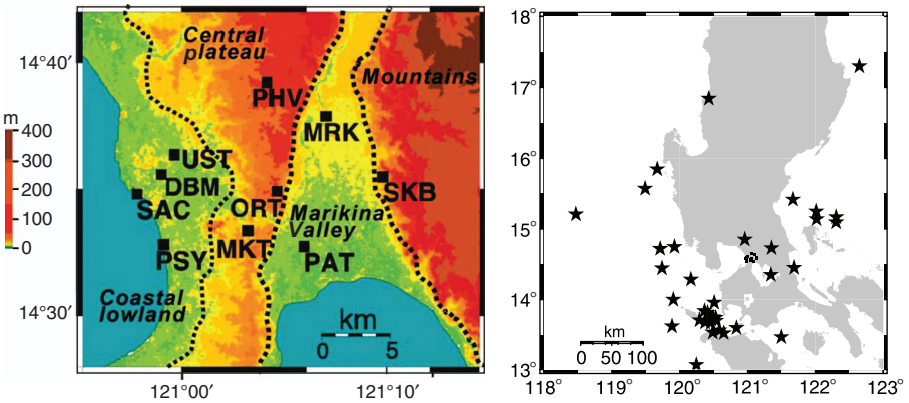

Fig. 1. Locations of earthquake stations (left) and epicentres of earthquakes (right) discussed in this study.

Table 1. List of earthquakes.

No.	Date	Local time	Lat. (deg)	Long. (deg)	Depth (km)	M
1	19991211	18:03:40	15.850	119.670	65	6.8
2	20000519	17:41:16	13.707	120.290	66	4.3
3	20000614	01:44:30	17.301	12.265	42	5.7
4	20000619	01:59:32	16.845	120.429	1	5.7
5	20000801	07:10:50	15.099	122.305	81	5.7
6	20001129	01:48:46	13.741	120.531	108	4.8
7	20010708	17:17:31	13.594	120.835	8	5.0
8	20010723	13:23:05	13.837	120.365	92	4.1
9	20011122	10:34:56	13.674	120.372	65	4.8
10	20011214	05:08:27	13.669	120.457	67	4.0
11	20020805	16:34:51	14.748	119.922	72	4.2
12	20020903	14:23:46	13.522	120.649	1	5.7
13	20020906	19:35:04	14.724	119.712	50	3.5
14	20020919	23:56:32	13.465	121.498	12	4.4
15	20021012	23:43:12	15.211	118.472	42	5.2
16	20021111	08:57:39	14.451	121.686	15	4.0
17	20021129	18:53:39	15.252	122.012	5	3.8
18	20030302	17:57:27	15.420	121.67	5	5.0
19	20030412	13:42:18	13.715	120.467	107	5.3
20	20030422	03:14:41	14.854	120.958	20	2.8
21	20030612	18:43:29	13.067	120.244	3	5.2
22	20330904	06:04:22	14.732	121.352	5	2.7
23	20031027	07:17:23	15.144	122.019	1	3.2
24	20031102	00:21:43	14.000	119.905	72	3.4
25	20040328	13:21:43	15.172	122.308	30	4.8
26	20040915	19:10:48	14.284	120.166	91	6.2
27	20041008	14:36:06	13.815	120.413	94	6.2
28	20041226	20:08:32	14.444	119.740	39	4.7
29	20050127	06:13:00	15.577	119.490	17	4.3
30	20050129	09:07:19	13.745	120.491	96	4.0
31	20050209	20:59:53	13.699	120.535	89	5.4
32	20050403	01:41:31	13.558	120.584	95	5.3
33	20050414	16:25:15	13.618	119.886	12	4.7
34	20050419	00:31:42	13.957	120.508	153	3.9
35	20050610	01:24:59	14.350	121.344	4	2.5
36	20051027	15:19:08	13.530	120.468	7	4.1

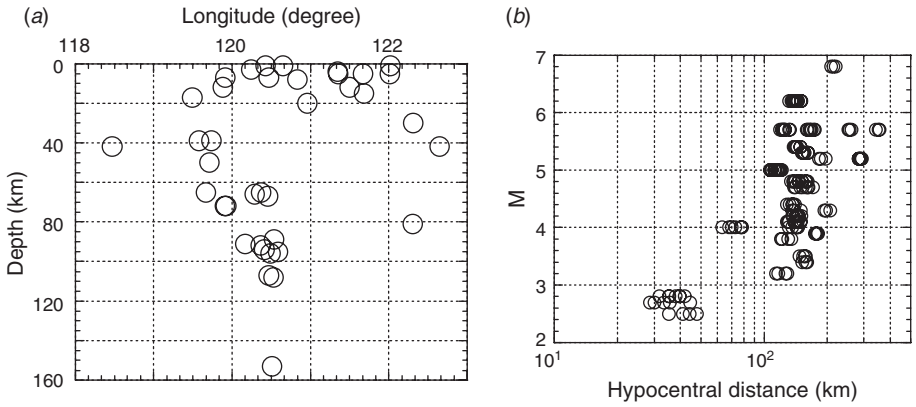

Fig. 2. Characteristics of earthquakes in this study. (*a*) Distribution of focal depths of earthquakes along the east–west direction. (*b*) Relationship between magnitudes of the earthquakes and hypocentral distances.

motion at high frequency. Therefore, the usual spectral ratio technique for estimation of empirical amplification is not used in this study. The S-wave velocity model for the shallowest soils was examined for use as a constraint condition. Figure 6 shows the observed S-wave spectra at the SKB site. Each spectrum is normalised by its maximum value. All the spectra exhibit common features, characterised by a dominant peak at a frequency of ~10 Hz. The theoretical amplification for the 1D model of the layers, over a basement with an S-wave velocity of 3 km/s, is also shown in the figure. This amplification is also normalised in the figure to compare with the observed spectra. The agreement with the existence of a distinct peak at a frequency of 10 Hz clearly indicates the appropriateness of the use of the 1D amplification for the constraint condition in the subsequent spectral inversion.

Q value for propagation path and source effects

Using the abovementioned constraint condition, we separated the effects of sources, Q value in the propagation path, and local site

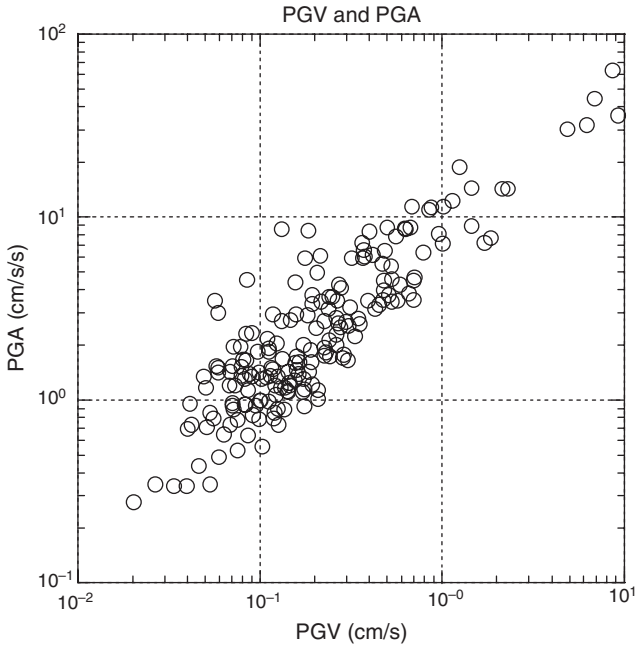

Fig. 3. Relationship between peak acceleration and velocity of earthquake records in this study.

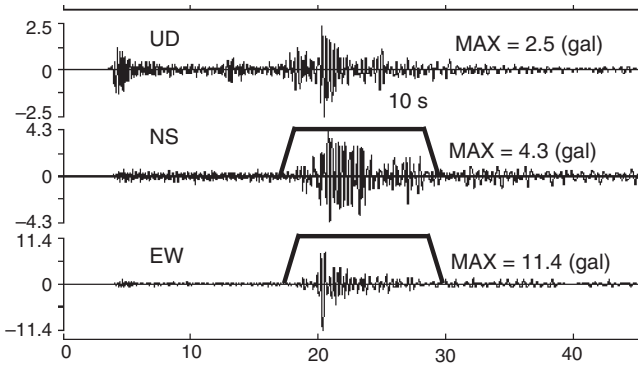

Fig. 4. Example of earthquake records obtained at PSY during event No. 9 in Table 1. A window with duration of 10 s is used in calculating S-wave spectra.

amplifications. The estimated Q values are shown in Figure 7. The Q value estimates vary smoothly across the range of frequencies of interest in this study. The solid line in the figure is a regression line for $Q = 50.6f^{1.1}$. Besana et al. (1997) estimated that a Q value for the crust and mantle in southern Luzon Island is 400 at a frequency of 1 Hz. This value is significantly different from our results. Since the ground motion data in our analysis includes the

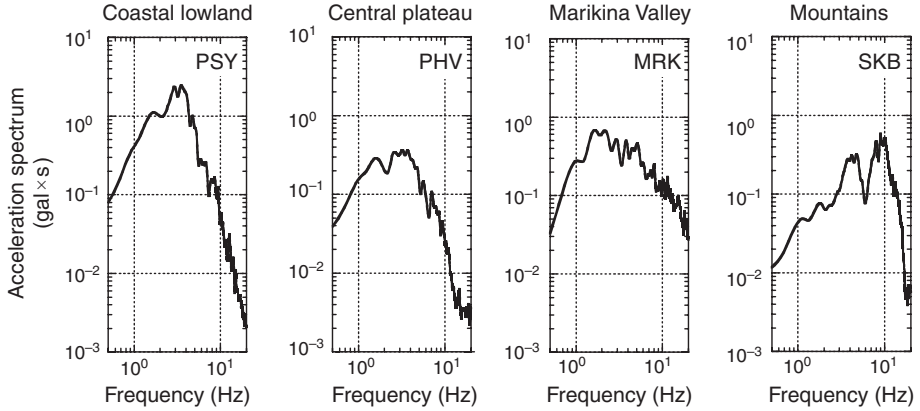

Fig. 5. Examples of Fourier spectra of S-wave part of earthquake records.

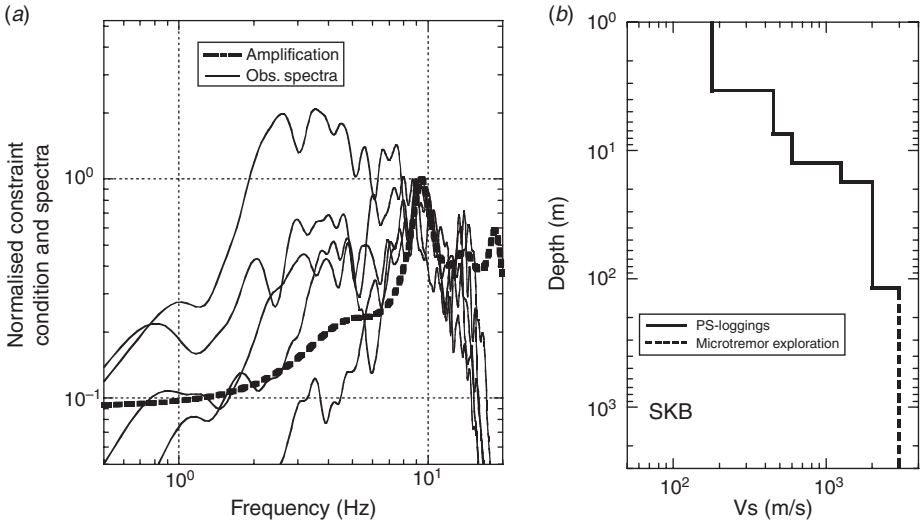

Fig. 6. Constraint conditions in spectral inversion. (*a*) Normalised Fourier spectra of S-waves at SKB (solid lines) and normalised S-wave amplification (a broken line) for (*b*) S-wave velocity model.

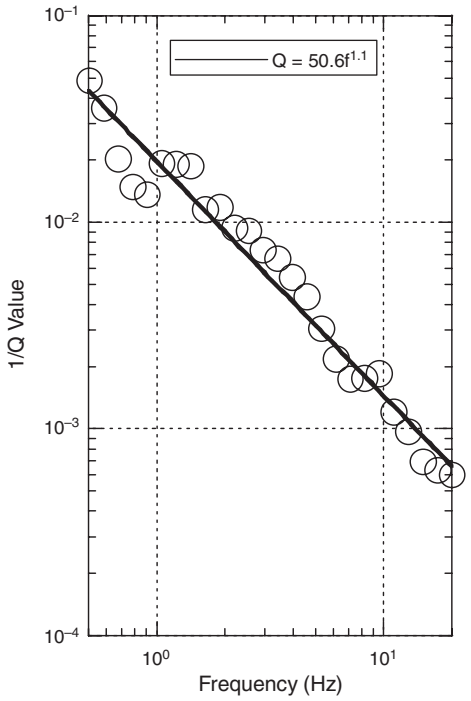

Fig. 7. *Q* value for propagation path estimated from spectral inversion.

records from the shallow earthquakes, the small *Q* values in our study are attributed to the attenuation characteristics for the shallow part of the crust.

Some examples of the source spectra with different magnitudes of earthquakes are depicted in Figure 8. The spectral amplitudes vary with the magnitudes. Source spectra for the omega-square models of Brune (1970), fitted to the observed spectra, are also shown by solid lines in Figure 9. Spectra for earthquakes with magnitudes less than 3 can be well approximated with the omega-square model. The model can also fit the observed source spectra for larger events, for frequencies below ~6 Hz, as can be seen in the figure.

Local site amplifications

The local amplification factors at all the sites are shown in Figure 10. The site amplifications in the coastal lowland, except for the UST station, show dominant peaks at a frequency of 1 to 2 Hz, with amplification factors of more than 10. The frequency of peak amplification at UST is higher than at the other three sites in the coastal area. Since UST is located near the boundary of the central plateau, the higher-frequency dominant peak is due to the shallower depth to firm soils. It is also noted that the peak amplitude at UST is almost the same as those for the other three sites, indicating the existence of a layer having similar S-wave velocity near the surface. Furthermore, all the amplification spectra at the sites in the coastal area have the common feature of a spectral decrease at higher frequencies. Shallow soils with a low S-wave velocity are responsible to the high-frequency decrease of the amplification, probably due to attenuation effects.

The amplification factors at the two sites in Marikina Valley are similar to those in the coastal area. The amplification spectrum at PAT is characterised by a dominant peak at the low frequency of 1.5 Hz, and decreasing amplitudes at frequencies above 8 Hz. However, the amplification spectrum at MRK does not show any decrease in amplitude at high frequencies. This clearly indicates that thick soft layers do not exist at MRK.

The amplification spectra at the three sites in the central plateau show relatively flat spectral features without any dominant peaks. The amplification factors are smaller than those in the coastal area and Marikina Valley, because of the absence of soft soils with a low S-wave velocity near the surface. It therefore follows that the amplification factors for these two sites can be mainly attributed to deep soils over the basement with an S-wave velocity of 3 km/s.

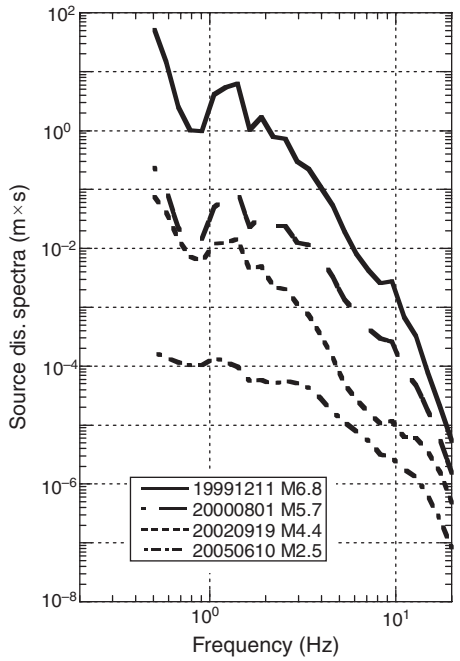

Fig. 8. Examples of source displacement spectra at distance of 1 km from spectral inversion.

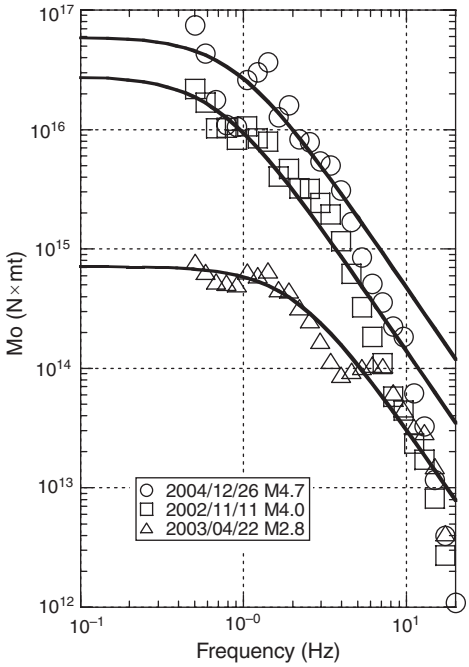

Fig. 9. Examples of source spectra and approximated omega-squared model shown by solid lines.

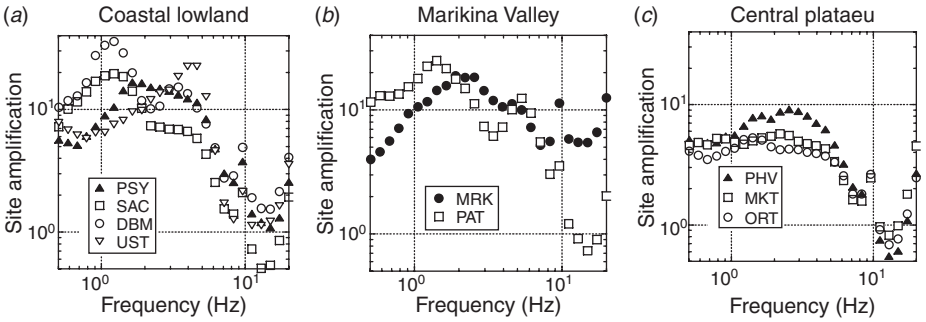

Fig. 10. Site amplification factors estimated from inversion of S-wave spectra at earthquake observation sites in (*a*) coastal lowland, (*b*) Marikina Valley and (*c*) central plateau.

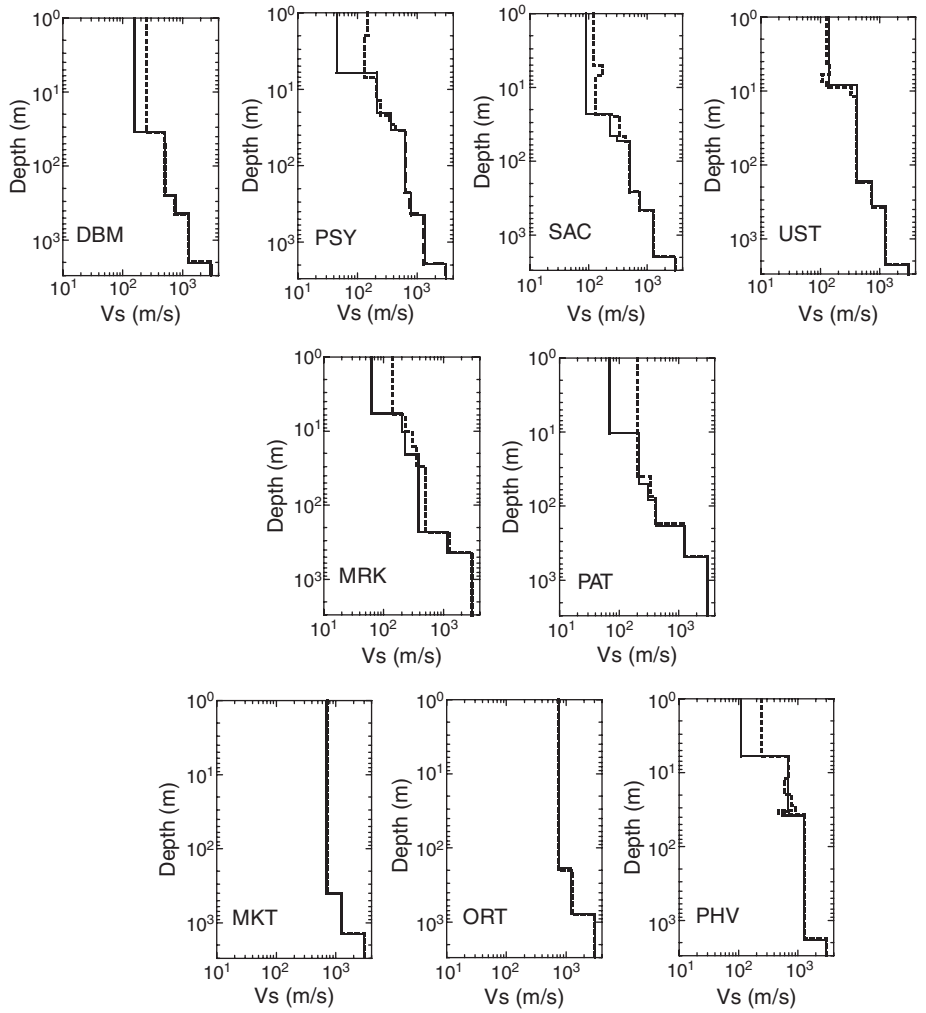

Fig. 11. S-wave velocity profiles at earthquake observation stations. Solid and broken lines indicate S-wave velocity models from inversion and available data, respectively.

Estimation of Vs profiles from site amplifications

In this section, we estimate an S-wave velocity profile at each earthquake observation site, using the amplification factors estimated from the spectral separation technique. First, we indicate the need to revise S-wave velocity profiles by comparing the amplifications with those calculated from existing S-wave velocity data. Then, we invert the amplification factors to new S-wave velocity profiles that are used for further investigation of the relationship between the amplifications and S-wave velocity distributions.

S-wave profiles from existing data

The amplification spectra estimated above are due to the effects of shallow and deep soils over a basement with an S-wave velocity of 3 km/s. Therefore S-wave velocity models for the shallow and deep soils were constructed from available data. Yamanaka et al. (2002*b*) conducted PS-logging at some of the observation stations in this study to determine S-wave velocity profiles for the soils down to a depth of ~100 m. S-wave velocity profiles for the deeper soils over the basement at some of the earthquake observation

stations were also revealed using microtremor exploration (Yamanaka et al., 2002*b*). Using their results, Yamada et al. (2003) also made a 3D S-wave velocity model for the deep soils in the area.

The S-wave velocity profiles at the nine stations are shown with broken lines in Figure 11. Note that the S-wave velocity and depth in the figure are shown with a logarithmic scale in order to express the wide ranges of the two parameters. There are no shallow S-wave profiles at MKT and ORT from PS-logging, because these stations are located in the central plateau with no thick soft soils near the surface.

The amplifications from the spectral inversion were compared with the theoretical 1D amplifications of S-waves propagating vertically in the S-wave profiles, shown by broken lines in Figure 11. Frequency-independent Q values were assumed for each layer, and assigned values equal to one-tenth of the S-wave velocity in m/s (e.g. Shibuya, 1983), because there is no detailed data for frequency characteristics of Q values in soils in these areas. The theoretical and observed amplifications are compared in Figure 12. The observed amplifications are larger than those calculated from the 1D S-wave models, indicated by broken lines. Furthermore, the periods of the observed peak amplifications are slightly longer than those of the calculated ones. It is, however, noted that the differences between the observed and theoretical amplifications are less at the stations in the central plateau (MKT and ORT), where there are no shallow low-velocity layers. These results suggest that the shallow soil layers can be one of the major reasons for the misfit between the observed and calculated amplifications. As explained above, the S-wave velocity of the near-surface soils were estimated from the results of S-wave logging near the stations. However, the distances between the boreholes and the strong-motion stations are more than 50 m at some of the sites. The difficulty of determining an accurate S-wave velocity in the top several metres from PS-logging is another reason for the inappropriateness of the S-wave velocity models. Therefore, the S-wave velocity models used here must be reconstructed.

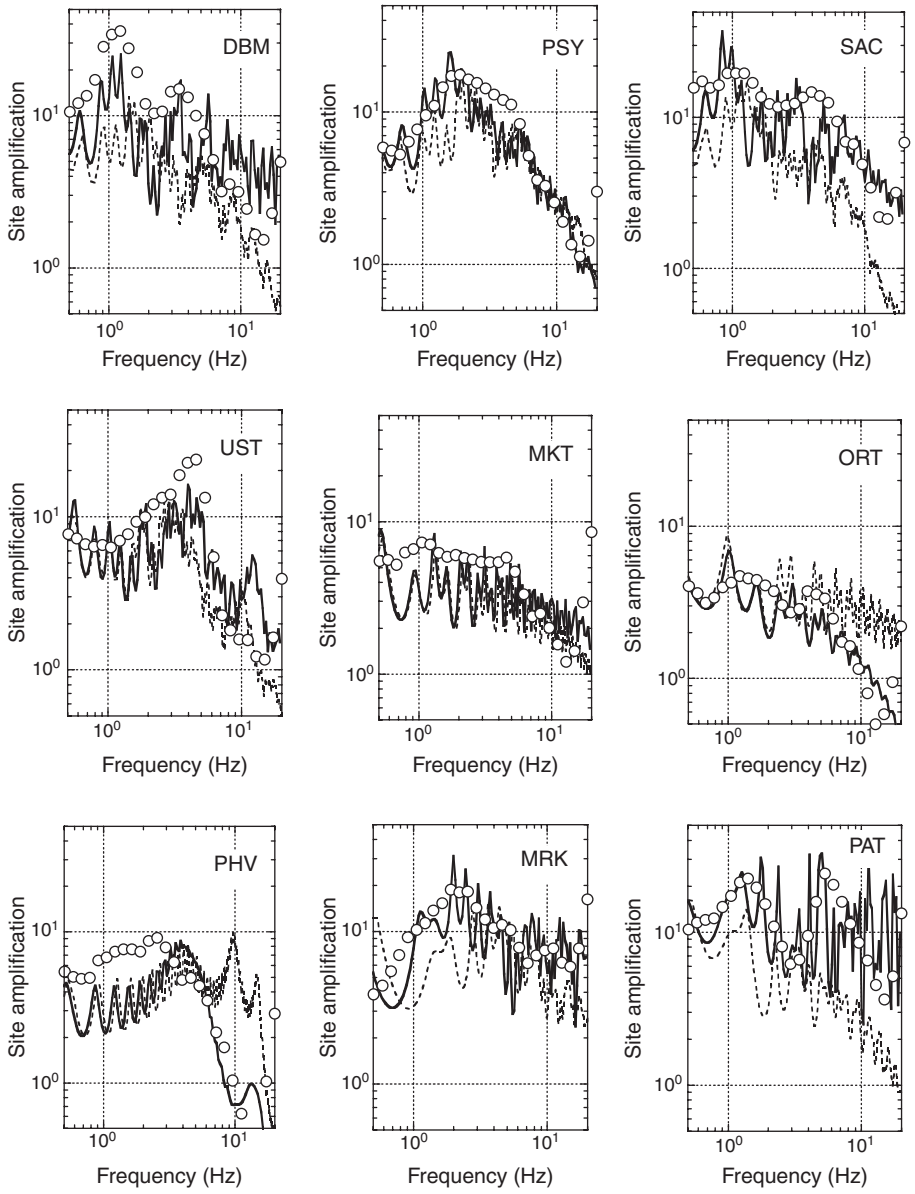

Fig. 12. Comparison of observed site amplifications (circles) with calculated amplifications of S-waves for S-wave profiles from available data (broken lines) and inverted S-wave profiles (solid lines).

Revision of S-wave profiles

The S-wave velocity models are modified to fit the observed amplifications with the theoretical ones. We used the following misfit measure:

$$misfit = \sum_{i=1}^{N} [G^0(f_i) - G^c(f_i)]^2.$$

The parameters controlling the amplification factors are S-wave velocity, thickness, density and Q value for each layer. The Q value is modelled from the S-wave velocity using the following relation (Satoh, 2003):

$$Q = \frac{\mathrm{Vs}}{b} f^a,$$

where a and b are constants determined in the inversion of the amplification factors together with S-wave velocity and thickness. We assumed that the constants, a and b, are common to all the layers at a site. We used a simulated annealing to minimise the misfit. The details of the simulated annealing can be seen in Yamanaka (2005).

In the inversion of the amplification factors, we assumed the same layering as the S-wave velocity profiles made from the available data in Figure 11. In particular, the search areas for the thicknesses are set to be narrower than those for the S-wave velocity, because the thickness data from the PS-loggings is usually more accurate than S-wave velocity. The search limits of the parameters in the inversion of the amplification at MRK are shown in Table 2 as an example. Since the simulated annealing is a kind of Monte Carlo methods, the estimated parameters depend more or less on random numbers used in the inversions. We, therefore, executed the inversions 10 times using different initial numbers of a random number generator. The final inverted parameters were estimated from averaging the parameters of the models obtained from the 10 inversions.

The inverted S-wave velocity models at the nine sites are shown by solid lines in Figure 11. Most of the inverted S-wave profiles have smaller S-wave velocities at shallow depths than those of the original profiles. In particular, the PSY, SAC, PAT, and MRK sites have a very low S-wave velocity, less than 100 m/s, in the top part of their models. However, the S-wave velocity structures for the deep soils are not so different from each other. The average values for the parameters for the Q values of the sediments, a and b, are estimated as shown in Table 3. Although it is quite difficult to find a regionality in the value of a, the b-values in the coastal area and the Marikina Valley are smaller than that for the central plateau. The observed and calculated amplifications

Table 2. Search limits of parameters in inversion of amplification at MRK.

Layer	Vs (m/s)	Thickness (m)	Density (t/m^3)	b	a
1	40–240	5–7	1400	5–50	0–2
2	130–330	3–5	1500		
3	200–500	9–11	1700		
4	300–600	184–224	1800		
5	1140–1400	180–220	2300		
6	3000	–	2500		

Table 3. Coefficients of Q values for inverted models [$Q=(V_s/b)f^a$].

	a	b
Coastal lowland	0.07	7.5
Marikina Valley	1.04	9.4
Central plateau	0.01	29.6

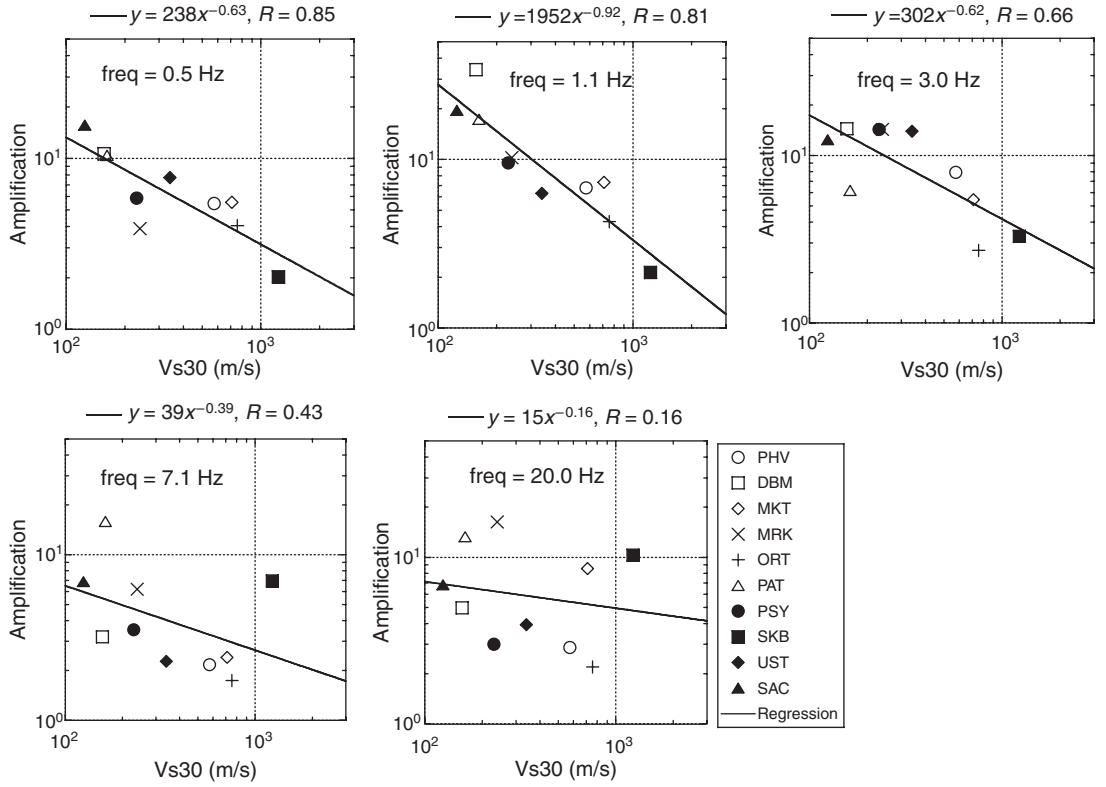

Fig. 13. Comparisons of amplifications with average S-wave velocity in top 30 m. R is correlation coefficient for a regression line shown in the top of each figure.

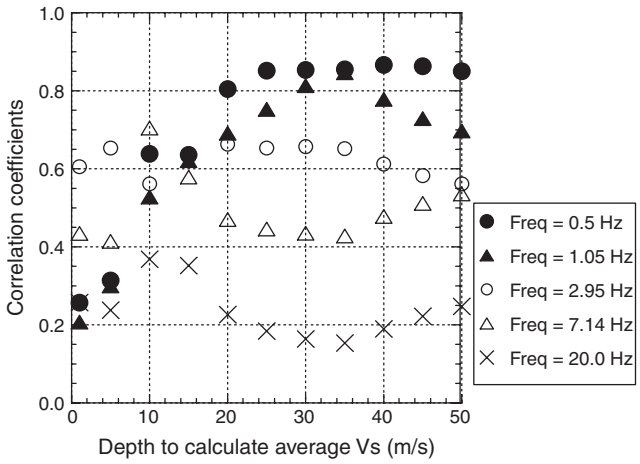

Fig. 14. Plot of correlation coefficients for relation between amplifications and average S-wave velocity with different depth for calculating the averages of S-wave velocity.

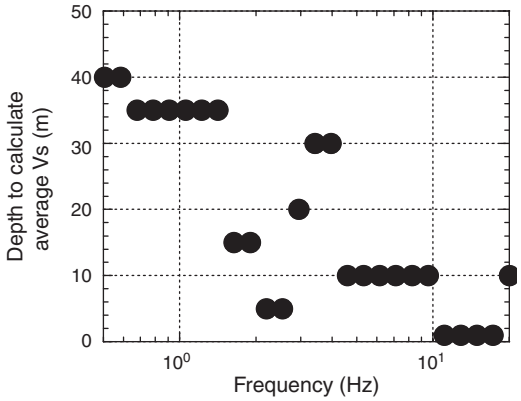

Fig. 15. Plot of depths to calculate average S-wave velocity with the maximum correlation against frequency.

are compared in Figure 12. The new inverted models can explain well the observed peak frequencies and amplitudes of the site effect spectra, which were difficult to explain with the original models. The amplifications at the sites in the central plateau are also well modelled at high frequency. However, we still have difficulty in explaining the amplification values at low frequency at PHV in the central plateau.

Relationship between AVS30 and amplification

In seismic microzonation, the average S-wave velocity in the top 30 m (AVS30) is often used to indicate local site conditions. We here discuss the relationship between the amplifications and the averaged S-wave velocity for the S-wave velocity profiles estimated in this study. Figure 13 shows examples of comparisons of the amplifications at some frequencies with the AVS30s of the inverted S-wave profiles. A regression line is also depicted in the figures. In the regression analysis, we assumed that the amplification is approximated with A*exp(-$AVS30$). This form of the equation is often used in previous studies on AVS30 (e.g. Midorikawa et al., 1994). The figures indicate that the correlation coefficients between the AVS30 and the amplifications are high at low frequencies, such as 0.5 and 1 Hz. This result agrees with previous investigations (e.g. Joyner and Fumal, 1984) indicating that the AVS30 measure is applicable to the assessment of local site amplification. Although the correlation coefficient becomes relatively low as 0.66 at a frequency of 3 Hz, we consider that the AVS30 is still a useful index with which to assess amplifications. However, the amplifications at the high frequencies of 7.1 and 20 Hz cannot be well explained by the AVS30 value as can be seen with low values of the correlation coefficient. This suggests that the high-frequency amplifications are not controlled by the effects of soils down to 30 m, but the effects of soils shallower than 30 m.

We, next, calculated the average S-wave velocities down to various depths in the inverted profiles, and compared them with the amplifications at each frequency. The correlation coefficients between the amplifications and the various averaged S-wave velocities were estimated in a similar way as is shown in Figure 13. The relationships between the depth over which the S-wave velocity is averaged and the correlation coefficients at various frequencies are plotted in Figure 14. The correlation coefficients at low frequencies of 0.5 and 1.0 Hz are almost constant for averaging depths greater than 25 m. However, the maximum correlation coefficients at higher frequencies are observed to occur at shallower S-wave velocity averaging depths. The averaging depths with the maximum correlation coefficients is plotted against a frequency in Figure 15. This clearly indicates that the amplifications at a higher frequency can be attributed to the soils at shallower depths than 30 m, and that the AVS30 measure is not sufficient for defining amplification at high frequency. In particular, the amplifications at frequencies more than 10 Hz are mostly controlled by the S-wave velocity at the surface.

It is noted that the amplifications estimated in this study are the effects of all the sedimentary layers over a basement with an S-wave velocity of 3 km/s. Therefore, the amplifications contain effects due to both shallow and deep soils. In the above discussions, we just took into account of the effects of shallow soils. We should consider the possibility that the relationship contains a bias due to the effects of deep soils.

Conclusions

In this study, we applied the spectral inversion technique to the S-wave spectra of earthquake records in metropolitan Manila, in the Philippines, in order to separate source, path and local site effects. The estimated Q value of the propagation path is modelled as $54.6f^{1.1}$. Most of the source spectra can be approximated with the omega-squared model. Site amplifications show different spectral features according to surface geological conditions. Amplifications at sites in the coastal lowland and the Marikina Valley show dominant peaks at frequencies from 1 to 5 Hz, while those in the central plateau show no dominant peaks. Amplifications at low frequency agree with those calculated using 1D S-wave velocity models from available geological and geophysical data. However, high frequency amplifications cannot be well explained by these models. These amplifications were inverted to new S-wave velocity profiles by fitting them with theoretical ones. We subsequently compared the amplifications with the average S-wave velocity in top 30 m of these S-wave profiles, and examined linear relationships between them at each frequency. It was found that the amplification at higher frequencies is attributed to soils at shallower depths than 30 m.

Acknowledgements

We thank Takao Kagawa and an anonymous reviewer for their comments that significantly improved the manuscript. We also thank Dr Lindsay Thomas for careful reading the manuscript and suggestions. The strong-motion data used in this study originated from a cooperative project between the Philippine Institute of Volcanology and Seismology and the Tokyo Institute of Technology, initially with a support of the Japan Society of Promotion of

Science. The authors acknowledge those who have been involved in the strong-motion observations at the two institutes.

References

Besana, G. M., Negishi, H., and Ando, M., 1997, The three-dimensional attenuation structures beneath the Philippine archipelago based on seismic intensity data inversion: *Earth and Planetary Science Letters*, **151**, 1–11. doi:10.1016/S0012-821X(97)00112-X

Brune, J., 1970, Tectonic stress and the spectra of seismic share waves from earthquakes: *Journal of Geophysical Research*, **75**, 4997–5009. doi:10.1029/JB075i026p04997

Daligdig, J.A., and Besana, G.M., 1993, Seismological hazards in Metro Manila: Natural Disaster Prevention and Mitigation in Metropolitan Manila area: Department of Science and Technology, Philippine Institute of Volcanology and Seismology, 9–41.

Daligdig, J.A., Punongbayan, R. S., Besana, G.M., and Tungol, N. M., 1997, The Marikina Valley fault system: Active faulting in eastern Metro Manila: PHIVOLCS professional paper, **1**, 1–20.

Gervasio, F. C., 1968, The geology, structures, and landscape development of Manila and suburbs: *The Philippine Geologist*, **22**, 178–192.

Iwata, T., and Irikura, K., 1986, Separation of source, propagation and site effects from observed S-waves: *Zisin (Journal of the Seismological Society of Japan)*, **39**, 579–593.[in Japanese with English Abstract]

Joyner, W. B., and Fumal, T. E., 1984, Use of measured shear wave velocity for predicting geologic and site effects on strong ground motion: Proceedings of the 8th World Conference on Earthquake Engineering, **2**, 777–783.

Kato, K., Takemura, M., Ikeura, T., Urao, K., and Uetake, T., 1992, Preliminary analysis for evaluation of local site effect from strong motion spectra by an inversion method: *Journal of Physics of the Earth*, **40**, 175–191.

Kurita, K., Yamanaka, H., Ohmachi, T., Seo, K., Kinugasa, Y., Midorikawa, S., Toshinawa, T., Fujimoto, K., and Abeki, N., 2000, Strong motion observation in Metro Manila, Philippines: The 12th World Conference on Earthquake Engineering, CDROM, No.1931.

Midorikawa, S., Matsuoka, M., and Sakugawa, K., 1994, Site effects on strong-motion records observed during the 1987 Chiba-ken-toho-oki, Japan, earthquake: Proceedings of the 9th Japan earthquake Engineering Symposium, 3, E085–E090.

Nelson, A. R., Personius, S. F., Rimando, R. E., Punongbayan, R. S., Tungal, N. M., Mirabueno, H., and Rasdas, A., 2000, Multiple large earthquakes in the past 1500 years on a fault in Metropolitan Manila, the Philippines: *Bulletin of the Seismological Society of America*, **90**, 73–85. doi:10.1785/0119990002

Philippine Institute of Volcanology and Seismology, 2004, Earthquake Impact Reduction Study for Metropolitan Manila, Republic of the Philippines, Final report, 2.7–2.8.

Satoh, T., 2003, Identification of damping factors from vertical array data considering obliquely incident S-waves: Application of simulated annealing method: *Journal of Structural and Construction Engineering*, **569**, 37–45.

Shibuya, J., 1983, Amplification of body waves, *in* Earthquake Motion and Ground Conditions: Architectural Institute of Japan, 98–105.

Takemura, M., Kato, K., Ikeura, T., and Shima, E., 1991, Site amplification of S-waves from strong motion records in special relation to surface geology: *Journal of Physics of the Earth*, **39**, 537–552.

Yamada, N., Yamanaka, H., Takezono, M., Kumada, C., and Baul-deocampo, J. R., 2003, Simulation of strong ground motion in Metro Mamina, the Philippines: *Journal of Structural Engineering. Architectural Institute of Japan*, **49B**, 1–6.[in Japanese]

Yamanaka, H., Nakamaru, A., Kurita, K., and Seo, K., 1998, Evaluation of site effects by an inversion of S-wave spectra with a constraint condition considering effects of shallow weathered layers:: *Zisin (Journal of the Seismological Society of Japan)*, **51**, 193–202. [in Japanese with English Abstract]

Yamanaka, H., Midorikawa, S., Kinugasa, Y., Bautista, B.C., and Rimando, R.E., 2002*a*, Estimation of Seismic Risk in Metro Manila, *in* Metro Manila, in Search of a Sustainable Future: University of the Philippines Press, 308–326.

Yamanaka, H., Yamada, N., Takezono, M., Baul-deocampo, J. R., Kumada, C., Tiglao, R. B., Bautista, B. C., Takahashi, Y., and Samano, T., 2002*b*, Exploration of sedimentary layers in Metropolitan Manila, the Philippines, for estimation of site effects: Proceedings of the 11th Japan Earthquake Engineering Symposium, 323–328. [in Japanese with English abstract]

Yamanaka, H., 2005, Comparison of performance of heuristic search methods for phase velocity inversion in shallow surface wave methods: *Journal of Environmental & Engineering Geophysics*, **10**, 163–173. doi:10.2113/JEEG10.2.163

Manuscript received 19 August 2010; accepted 7 November 2010.

フィリピン・マニラ首都圏での地震観測記録を用いた地盤増幅特性の評価とS波速度構造の推定

山中浩明[1]・太田原薫[1]・R.グルータス[1]・R.テグラオ[2]・M.ラサラ[2]・I.C.ナラグ[2]・B.C.バウティスタ[2]

1 東京工業大学大学院総合理工学研究科
2 フィリピン火山地震研究所

要　旨： フィリピン・マニラ首都圏では、東工大地震動研究のグループとフィリピン火山地震研究所によって強震観測網が構築され、10 地点での地震観測が続けられている。本研究では、この観測網で得られた中小地震（M2.5～6.8）の観測記録の S 波スペクトルを用いて、地盤増幅特性を求め、さらにその増幅特性の逆解析から S 波速度構造を推定することを試みた。地震記録の分析には、S 波スペクトルを伝播経路の Q 値、震源特性、および地盤増幅特性に分離するインバージョン方法を用いた。拘束条件として、岩盤サイトでの表層から地震基盤までの地盤構造モデルの 1 次元理論増幅特性を与えた。伝播経路の Q 値は、$Q=54.6f^{1.1}$ となった。震源スペクトルの多くは、ω2 モデルに近いものであった。一方、得られた地盤増幅特性には、この地域の３つの地形区分に対応した差異が認められた。すなわち、西側の海岸低地と東側のマリキナ低地での増幅特性には、１から 5Hz で明瞭なピークが認められた。一方、中央台地の観測点では、ほぼ平坦な地盤増幅特性が得られた。各観測点で得られた地盤特性が 1 次元理論地盤増幅特性と合うようにして、各地層の S 波速度、厚さ、Q 値を同定した。さらに、これらの同定した地盤モデルを用いて、深さ 30ｍまでの平均 S 波速度と周波数毎の増幅特性の相関を調べた。その結果、6Hz 程度までは平均 S 波速度と増幅特性は、線形式で近似できた。しかし、7Hz よりも高い周波数での増幅特性は、より浅い深さまでの平均 S 波速度との相関が高いことがわかった。とくに、10Hz 以上の増幅特性は、地表での S 波速度の値によってよく説明できた。

キーワード：地震観測，マニラ，地盤特性，S 波速度，Q 値，フィリピン

지진 관측 기록을 이용한 필리핀 마닐라의 현장 증폭 특성 및 S파 속도구조 추정

Hiroaki Yamanaka[1], Kaoru Ohtawara[1], Rhommel Grutas[1],
Robert B. Tiglao[2], Melchor Lasala[2], Ishmael C. Narag[2], Bartlome C. Bautista[2]

1 동경공업대학 대학원 종합이공학연구과
2 필리핀 화산 지진 연구소

요 약： 본 연구에서는, 필리핀의 마닐라에서 관측된 지진 기록을 통해 얇고 깊은 토양층의 S파 속도 구조 와 경험적 현장 증폭 특성을 평가하였다. 지진 기록에 빛띠 역산법(Spectral inversion technique)을 적용하여 진원, 경로 및 국지적 현장 증폭 효과들을 평가하였다. 사용한 지진 자료는 36회의 중간급 지진들의 기록을 얻었으며, 그 중에서 마닐라의 지진 관측 망에서 강한 움직임을 보인 10곳의 관측점 자료를 이용하였다. 전파경로의 추정 Q값은 54.6f 1.1으로 모사된다. 대부분의 진원의 빛띠(스펙트럼)는 오메가-스퀘어(omega-square) 모형으로 근사 될 수 있다. 현장 증폭 특성은 지표 지질조건에 따라 특유의 특징을 보여준다. 중앙 고지대의 증폭특성은 우세 주파수를 갖지 않는데 비해, 해안 저지대 와 마리키나(Marikina) 계곡에서의 증폭특성은 1~5Hz의 우세 주파수를 갖는다. 우리는 현장 증폭 특성을 S파 속도로 변환한 후에, 증폭 특성과 상부 30m의 평균 S파 속도 구조와의 관계를 검토하였다. 낮은 주파수대의 증폭 특성은 평균 S파 속도와 좋은 상관성을 보인다. 반면, 높은 주파수대의 증폭특성은 상부 30m내의 평균 S파 속도로 충분히 설명되지 않는다. 이것은 30m보다 낮은 심도의 평균 S파 속도와 더 많이 관련되어 있다.

주요어： 지진 관측, 마닐라, 현장 증폭, S 파 속도, Q 값, 필리핀